HHS Public Access

Author manuscript

Mol Neurobiol. Author manuscript; available in PMC 2018 December 01.

Published in final edited form as:

Mol Neurobiol. 2018 December ; 55(12): 9089–9099. doi:10.1007/s12035-018-1047-3.

MiR-34a Regulates Axonal Growth of Dorsal Root Ganglia Neurons by Targeting FOXP2 and VAT1 in Postnatal and Adult Mouse

Longfei Jia[1,2], **Michael Chopp**[1,3], **Lei Wang**[1], **Xuerong Lu**[1], **Yi Zhang**[1], **Alexandra Szalad**[1], and **Zheng Gang Zhang**[1]

[1]Department of Neurology, Henry Ford Hospital, 2799 West Grand Boulevard, Detroit, MI 48202, USA

[2]Department of Neurolgoy, Xuanwu Hospital, Capital Medical University, Beijing, China

[3]Department of Physics Oakland University, Rochester, MI 48309, USA

Abstract

Hyperglycemia impairs nerve fibers of dorsal root ganglia (DRG) neurons, leading to diabetic peripheral neuropathy (DPN). However, the molecular mechanisms underlying DPN are not fully understood. Using a mouse model of type II diabetes (db/db mouse), we found that microRNA-34a (miR-34a) was over-expressed in DRG, sciatic nerve, and foot pad tissues of db/db mice. In vitro, high glucose significantly upregulated miR-34a in postnatal and adult DRG neurons, which was associated with inhibition of axonal growth. Overexpression and attenuation of miR-34a in postnatal and adult DRG neurons suppressed and promoted, respectively, axonal growth. Bioinformatic analysis suggested that miR-34a putatively targets forkhead box protein P2 (FOXP2) and vesicle amine transport 1 (VAT1), which were decreased in diabetic tissues and in cultured DRG neurons under high glucose conditions. Dual-luciferase assay showed that miR-34a downregulated *FOXP2* and *VAT1* expression by targeting their 3′ UTR. Gain-of- and loss-of-function analysis showed an inverse relation between augmentation of miR-34a and reduction of FOXP2 and VAT1 proteins in postnatal and adult DRG neurons. Knockdown of FOXP2 and VAT1 reduced axonal growth. Together, these findings suggest that miR-34a and its target genes of *FOXP2* and *VAT1* are involved in DRG neuron damage under hyperglycemia.

Keywords

miR-34a; Axon growth; Neuron; Peripheral neuropathy

Correspondence to: Zheng Gang Zhang.

Conflict of Interest The authors declare that they have no conflict of interest.

Electronic supplementary material The online version of this article (https://doi.org/10.1007/s12035-018-1047-3) contains supplementary material, which is available to authorized users.

Introduction

Hyperglycemia induces axonal damage of dorsal root ganglia (DRG) neurons, leading to diabetic peripheral neuropathy (DPN) [1, 2]. Molecular mechanisms underlying distal axonal loss in DPN are not fully understood. Multiple mechanisms including polyol pathway, hexosamine and protein kinase C (PKC), advanced glycation end products, free fatty acids, ion conductance, mitochondrial dysfunction, insulin resistance and inflammation, have been well demonstrated preclinically in mediating the development of DPN [1–3]. However, clinical trials targeting these mechanisms have failed [1]. Increasing evidence shows that microRNAs (miRNAs), for example, miR-338, miR-16, miR181d, miR-132, miR-9, miR-17-92, and miR-29c, play critical roles in regulating axonal development [4]. In addition, miRNAs are involved in diabetes and diabetes-induced complications [5]. Mice with diabetic neuropathic pain exhibit reduction of miR-184 and miR-190a in spinal cord tissue [6], while diabetic rats showed downregulation of miR-29b in DRG neurons [7]. Moreover, miR-7a regulates excitability of DRG neurons in a neuropathic pain model [8], whereas miR-21 and miR-222 inhibit apoptosis of DRG neurons induced by sciatic nerve injured [9]. Although miR-34a has been well demonstrated to regulate cancer cell growth [10], recent studies show that patients with diabetes have high serum levels of miR-34a [11]. Experimental studies show that an increased miR-34a in islets is associated with the progression of the diabetes, and that fatty acids upregulate miR-34a expression in pancreatic β-cells [12, 13]. These data suggest that miR-34a may be involved in diabetic metabolic dysfunction. Moreover, miR-34a has been shown to regulate neurite outgrowth, spinal morphology and function [14]. However, the role of miR-34a in DPN remains unknown.

Here, using a mouse model of type II diabetes (db/db mice) and cultured DRG neurons, we report that hyperglycemia increases miR-34a in DRG neurons and suppresses axonal growth through regulating genes of *FOXP2* and *VAT1*. FOXP2 is a transcription repressor and regulates neurite growth during nervous system evolution [15]. VAT1 is a membrane protein of cholinergic synaptic vesicles [16]. The role of these two genes in DPN is not known. Our data for the first time suggest that miR-34a and its target genes *FOXP2* and *VAT1* are involved in DPN.

Research Design and Methods

All experimental procedures were conducted in accordance with the NIH Guide for the Care and Use of Laboratory Animals and approved by the Institutional Animal Care and Use Committee of Henry Ford Hospital.

Isolation of DRG, Sciatic Nerve and Foot Pad Tissues

DRG, sciatic nerve (SN) and foot pad (FP) tissues were harvested from BKS.Cg-m $^{+/+}$Lepr^{db}/J (db/db) mice (Jackson Laboratories, Bar Harbor, ME, USA) at the age of 20 weeks when mice exhibited peripheral neuropathy [17] (Fig s1). The db/db mouse has a point mutation in the leptin receptor gene causing severe depletion of the insulin-producing beta-cells of the pancreatic islets, hyperglycemia and eventually leading to diabetes [18].

The age-matched heterozygote mice (db/m) were used as control. Physiological parameters of db/m and db/db mice including blood glucose levels were measured (Fig s1).

Culture of Primary Postnatal and Adult DRG Neurons

DRG neurons were harvested from newborn C57L/J mice (Jackson Laboratories) at postnatal day 0–1 or adult (20 weeks) db/m and db/db mice and were cultured according to published protocols [19, 20]. Briefly, the DRGs were collected and then transferred into neurobasal medium (Invitrogen, Carlsbad, CA, USA) containing 0.25% trypsin (Thermo Fisher Scientific, Waltham, MA, USA) digestion at 37 °C for 30 min. DRG neurons were mechanically triturated with a Pasteur pipette for 15 times and then the cells were passed through a 70-μm cell strainer (Fisher Scientific, Hampton, NH, USA) and counted to obtain a concentration of 1×10^7 cells/ml.

Postnatal DRG neurons were cultured in a microfluidic chamber (Xona Microfluidics, Temecula, CA, USA). Microgrooves embedded in the chamber allow only axons to pass and reach the axonal compartment [20, 21]. Sterilized chambers were affixed to poly-D-lysine-coated (Sigma-Aldrich, St. Louis, MO, USA) dishes (35 mm, Corning, Corning, NY). Postnatal DRG neurons were cultured at a density of 1×10^6 cells/chamber, and adult DRG neurons were cultured at a density of 1×10^5 in DMEM (Thermo Fisher Scientific) with 5% FBS (Corning) for 4 h. Then the medium was replaced with neurobasal medium (Invitrogen), 50 ng/ml nerve growth factor (NGF) (Sigma-Aldrich), 2% B-27 (Invitrogen), 2 mM GlutaMax (Thermo Fisher Scientific), and 1% antibiotic-antimycotic (Thermo Fisher Scientific). The 5-fluorodeoxyuridine (Abcam, Cambridge, UK) was added to purify the neurons. The medium was changed with non-5-fluorodeoxyuridine neurobasal medium on day in vitro (DIV) 3. Then, the medium was replaced every other day. Additional 5 mM glucose was added into the neurobasal medium containing 25 mM glucose to reach a final concentration of 30 mM glucose that has been shown to be the optimal condition for culturing DRG neurons [22]. To induce a high glucose (HG) condition, additional 30 mM glucose was applied into the neurobasal medium. In the present study, we thus termed 30 and 55 mM glucose media as regular glucose (RG) and HG, respectively.

Transfection of DRG Neurons

Postnatal and adult DRG neurons were transfected with miR-34a mimics, miR-34a hairpin inhibitors, and their corresponding controls (Dharmacon, Lafayette, CO, USA) using Nucleofector™ kit (Lonza, Basel, Switzerland). Briefly, 200 pmol/well of miRNA mimics and inhibitors were mixed with 100 μl of Nucleofector solution (Lonza). Then, DRG neurons with the transfection solution were transferred into a cuvette. The program O-03 was used for electroporation [23]. SiRNAs against *FOXP2* and *VAT1*, or controls (0.1 μM, Santa Cruz, Santa Cruz, CA, USA) were transfected using the same protocol.

Isolation of Total RNA and Real-Time RT-PCR Analysis

MiRNeasy Mini kit (Qiagen, Hilden, Germany) was used to isolate total RNA from cultured DRG neurons (DIV6), or tissues of DRGs, sciatic nerves and foot pads of db/db and db/m mice. Quantitative RT-PCR (qRT-PCR) analysis was performed on ABI 7000 and ABI ViiA 7 PCR instrument (Applied Biosystems, Foster City, CA, USA) according to published

methods [24, 25]. The following miRNA primers were used: miR-34a (mature sequence: UGUUGGUCGAUUCUGUGACGGU) and U6 snRNA (mature sequence: GTGCTCGCTTCGGCAGCACA TATACTAAAATTGGAACGATACAGAGAAGATTAGCA TGGCCCCTGCGCAAGGATGACACGCAAATT CGTGAAGCGTTCCATATTTT). Briefly, for the reverse transcription, 15 μl of reverse transcription reactions were used, consisting of 1–10 ng total RNA, 5 U MultiScribe Reverse Transcriptase (Applied Biosystems), 0.5 mM each of dNTPs (Applied Biosystems), 1× reverse transcription buffer (Applied Biosystems), 4 U RNase inhibitor (Applied Biosystems), and nuclease-free water (Applied Biosystems). The running program was as follows: 16 °C for 30 min, 42 °C for 30 min, 85 °C for 5 min. Twenty μl qRT-PCR reactions were used, consisting of 1×TaqMan Universal PCR Master Mix No AmpErase UNG, 1× TaqMan miRNA assay, 1.33 μl of undiluted cDNA and nuclease-free water. The running program was 95 °C for 10 min, followed by 40 cycles at 95 °C for 15 s, and 60 °C for 1 min. Each sample obtained from at least three independent experiments was tested in triplicate. Relative levels of miRNAs were calculated by means of the formula $2^{-\Delta\Delta C_T}$ after normalizing $\Delta\Delta C_T$ values to a reference snRNA U6. CT values and melt curve were checked. The method of $2^{-\Delta\Delta C_T}$ was used to calculate the relative levels [26].

Dual-Luciferase Assay

Dual-Luciferase assay was performed according to our published protocol [27]. Briefly, the segments of the 3′ UTR of *FOXP2* (MmiT037037, Genecopoeia, Rockville, MD, USA) and *VAT1* (MmiT030775, Genecopoeia) gene encompassing the miR-34a binding site were cloned into a pEZX-MT06 vector with Firefly/Renilla duo Luciferase reporter driven by a CMV promoter (Genecopoeia) (Fig. 6b). Mutations of 3′ UTR in miR-34a binding site of *FOXP2* (ACTGCCA to TACCAGC) and *VAT1* (CACTGCCA to GCCACACT) gene were made, and confirmed by sequencing (Fig.6b). Wild-type or mutant vectors were transfected into HEK293 cells by lipofectamine (Life technologies, Carlsbad, CA, USA) at a concentration of 2 μg/106 cells. To test the interaction between miR-34a and 3′ UTR of *FOXP2* or *VAT1* gene, each vector was co-transfected with miR-34a mimics (200pM/10^6 cells, Dharmacon). Twenty-four hours later, HEK293 cells were lysed and treated with a Dual-luciferase assay kit (Genecopoeia). Luciferase activity was measured by multimode microplate reader (PerkinElmer/Fusion).

Western Blot Analysis

Total proteins from cultured DRG neurons were isolated on DIV6 according to published protocols [25, 27]. Total protein from DRG, sciatic nerve and foot pad tissues of db/db and db/m mice were extracted using the same methods. In vitro samples from 4 individual microfluidic chambers were pooled for one Western blot. The protein concentration was measured using a bicinchoninic acid protein assay kit (Thermo Fisher Scientific). Western blot was performed according to previously described methods [25, 27]. Briefly, equal amounts of proteins were loaded. Primary antibodies were rabbit anti-ADAM10 (a disintegrin and metalloproteinase domain-containing protein 10, 1:1000, Abcam, Cambridge, UK), rabbit anti-DCX (doublecortin, 1:500, Abcam), rabbit anti-c-MET (tyrosine-protein kinase met, 1:500, Abcam), rabbit anti-FOXP2 (1:1000, Abcam), goat anti-NOTCH1 (1:1000, Santa Cruz), rabbit anti-ROCK1 (Rho associated coiled-coil containing protein kinase 1, 1:500, Abcam), rabbit anti-SYNJ1 (Synaptojanin 1, 1:1000, Sigma-

Aldrich), rabbit anti-VAMP2 (vesicle-associated membrane protein 2, 1:1000, Cell Signaling Technology, Danvers, MA, USA), goat anti-VAT1 (1:1000, Santa Cruz), and mouse anti-β-actin (1:10000; Abcam). The optical density of protein bands was measured and calculated by means of Fluorchem E instrument (ProteinSimple, San Jose, CA, USA).

Immunofluorescent Staining and Axonal Measurement

Axonal staining and measurement were performed as previously described [20, 23]. Briefly, monoclonal antibodies against phosphorylated neurofilament heavy protein (SMI31, 1:1000, Covance, Battle Creek, MI, USA) or class III beta-tubulin (TUJ1, 1:1000, Biolegend, San Diego, CA, USA) were used. For postnatal DRG neurons, the lengths of the 15 longest axons in each chamber were measured using a microscopic computer imaging device (MCID) system. The axonal length was recorded for 3 days from DIV3 to DIV5. For adult DRG neurons, one time point axonal length was measured on DIV3 according to a published protocol [28]. Immunostaining for DRG tissues was performed according to a published protocol [24]. Briefly, L3–L6 DRGs were isolated, fixed in 4% paraformaldehyde, and embedded in paraffin. The slices were cut in 6 μm thickness. The following primary antibodies were used: rabbit anti-FOXP2 (1:50, Abcam) and goat anti-VAT1 (1:50, Santa Cruz). Cellular nuclei were stained with 4′,6-diamidino-2-phenylindole (DAPI) (1:10000, Thermo Fisher Scientific). A polyclonal antibody against protein gene product 9.5 (PGP 9.5, 1:1000; Millipore) was used to detect intraepidermal nerve fibers in plantar skin. The nerve fiber densities were calculated according to a published protocol [29].

Fluorescence In Situ Hybridization

Fluorescence in situ hybridization (FISH) in combination with fluorescent immunostaining were performed according to a published protocol [30]. Briefly, the cells were fixed in 4% paraformaldehyde, and then hybridized with a miR-34a LNA (locked nucleic acid) probe, and the probe was detected with peroxidase-conjugated anti-FAM (Roche, Basel, Switzerland) followed by incubation tyramine-signal-amplification (TSA)-Cy3 substrate for 10 min at room temperature. Fluorescent immunostaining was then performed with primary antibodies against TUJ1 (a marker of neuroblasts) and FITC-conjugated secondary antibody (Jackson ImmunoResearch, West Grove, PA, USA).

Bioinformatic Analysis

Bioinformatics were analyzed using TargetScan [31], Ingenuity Pathways Analysis (IPA) and string-db.org. For IPA, Fischer's exact test was used to calculate the *P* value.

Statistical Analysis

Data were analyzed by using SPSS 11.5. One-way ANOVA with post hoc Bonferroni tests was used for multiple group experiment analysis. Student's test was used for two group comparisons. A value of $P < 0.05$ was considered as significant. Values are presented as mean ± standard deviation (SD).

Results

MiR-34a Is Increased in Diabetes and Regulates Axonal Growth

To examine whether diabetes affects miR-34a expression, we measured miR-34a levels in DRG, sciatic nerve and foot pad tissues by means of qRT-PCR. Our data showed that miR-34a levels were significantly ($p < 0.05$) increased in DRG (1.9 ± 0.2 vs 1.0 ± 0.1, mean ± SD, $n = 6$), sciatic nerve (2.1 ± 0.3 vs 1.0 ± 0.2, n = 6) and foot pad (1.9 ± 0.2 vs 1.1 ±0.2, n= 6) tissues of diabetic db/db mice at age of 20 weeks compared to those of age- matched non-diabetic db/m mice (Fig. 1a). In vitro experiments showed that miR-34a levels were also increased in postnatal (2 ± 0.3 vs 1.0 ± 0.1, n=6, $P < 0.05$) and adult DRG neurons (2.8 ± 0.4 vs 1.0 ± 0.1, n = 6, $P < 0.05$) under HG conditions (Fig. 1b). In situ hybridization further confirmed that miR-34a increased in DRG neurons under HG conditions (Fig. 2a, b). We then assessed the role of miR-34a in axonal growth by transfecting postnatal DRG neurons with miR-34a inhibitors or mimics under HG conditions (Fig. 1c-d). The efficacy of transfection was confirmed by qRT-PCR analysis showing that miR-34a inhibitors and mimics reduced and increased, respectively, miR-34a levels in DRG neurons (Fig. 1b). To examine the effect of alteration of miR-34a levels on axonal growth, transfected postnatal DRG neurons were cultured in the microfluidic device and distal axonal length within the axonal compartment was measured. Our pilot experiments demonstrated that axons of postnatal and adult DRG neurons were SMI31 and TUJ1 immunoreactive, and double immunofluorescent staining showed co-localization of SMI31 and TUJ1 (Fig. s2), which is consistent with data from others [32]. Thus, SMI31 or TUJ1 positive axons were used for measurements of axonal length. As we expected, HG substantially reduced axonal length by 22% on DIV 5 compared to RG (Fig. 1c, d). However, miR-34a inhibitors completely suppressed HG-reduced axonal length, whereas miR-34a mimics further significantly ($p < 0.05$) decreased HG-reduced axonal length (Fig. 1c, d). To examine the effect of miR-34a on adult DRG neurons, transfected DRG neurons were cultured in regular dishes due to technical challenges to culture adult DRG neurons in the microfluidic device. In line with the data from postnatal DRG neurons, HG reduced axonal length by 58%, which was completely suppressed by miR-34a inhibitors and was further substantially ($p < 0.05$) decreased by miR-34a mimics (Fig. 1e, f). These data suggest that miR-34a regulates axonal growth of postnatal and adult DRG neurons.

FOXP2 and VAT1 Are Involved in MiR-34a-Mediated Axon Growth under Hyperglycemia Condition

In our preliminary studies, we examined protein levels of *ADAM10*, *DCX*, *c-MET*, *NOTCH1* and *ROCK1* genes putatively targeted by miR-34a, based on bioinformatic analysis. These genes are highly involved in pathways that are related to development of neurons, neuritogenesis, and branching and growth of neurites (Fig. s3a-d). However, Western blot analysis showed that none of these protein levels were altered in DRG, SN and FP tissues of db/db mice compared to db/dm mice (Fig. s4a-j). Thus, we searched other miR-34a putative target genes associated with the nervous system and found *SMAD4*, *FOXP2*, *SYNJ1*, *VAMP2* and *VAT1* genes. Among them, we detected reduction of FOXP2 and VAT1 proteins in diabetic mice (Fig. 3a-e). Thus, we focused on these two genes. Western blot analysis of DRG, SN and FP tissues from db/db and db/m mice showed that

FOXP2 and VAT1 protein levels were significantly reduced in DRG by 48% and 45%, respectively, SN by 38% and 48%, respectively, and FP 45% and 42%, respectively, tissues of db/db mice compared to protein levels in db/m mice (Fig. 3a-e).

Moreover, compared to RG conditions, HG significantly ($p < 0.05$) reduced FOXP2 and VAT1 proteins in cultured postnatal and adult DRG neurons (Fig. 4a, b). An inverse relation between augmentation of miR-34a and reduction of FOXP2 and VAT1 proteins suggests that miR-34a could target these two genes in DRG neurons. We thus performed in vitro experiments to assay the direct effect of miR-34a on *FOXP2* and *VAT1* genes using a dual-luciferase reporter approach, in which HEK293 cells were transfected by a plasmid containing miR-34a binding site at 3'UTR of *FOXP2* and *VAT1* genes (Fig. 4c). The luminescence analysis showed that miR-34a mimics significantly ($p < 0.05$) reduced luminescence activity of *FOXP2* or *VAT1* vector by 62% or 70%, respectively (Fig. 4d-e). In contrast, miR-34a mimics did not reduce luminescence activities when miR-34a seed sequences at 3' UTR of *FOXP2* or *VAT1* were mutated (Fig. 4d-e). Furthermore, transfection of postnatal and adult DRG neurons with miR-34a mimics or inhibitors resulted in decreases or increases, respectively, of FOXP2 and VAT1 protein levels in DRG neurons (Fig. 4f-h). Collectively, these data indicate that miR-34a regulates expression of *FOXP2* and *VAT1* by targeting their 3'UTR.

To examine whether FOXP2 and VAT1 regulate axonal growth, we transfected postnatal and adult DRG neurons with siRNAs against FOXP2 or VAT1 and then cultured transfected DRG neurons under RG conditions. Western blot analysis showed that siRNAs against FOXP2 or VAT1 significantly ($p < 0.05$) reduced FOXP2 or VAT1 levels in DRG neurons (Fig. 5a,b and Fig. 6a,b). Knockdown of endogenous FOXP2 or VAT1 robustly ($p < 0.05$) reduced axonal growth by 23% and 20% in postnatal neurons, or by 29% and 26% in adult neurons, respectively, compared to the controls (Fig. 5c-f and Fig. 6c-f), suggesting that FOXP2 and VAT contribute to axonal growth of DRG neurons.

Discussion

We have demonstrated that miR-29c mediates axonal growth of DRG neurons under hyperglycemia via targeting a gene that encodes a member of the protein kinase C (PKC) iota, *PRKCI* [33]. Here, we show that hyperglycemia upregulates miR-34a in DRG neurons. Importantly, we show that an increased miR-34a suppresses axonal growth by targeting *FOXP2* and *VAT1* genes. Together, these findings suggest that miRNAs mediate diabetes-induced axonal damage of DRG neurons.

Degeneration of distal sensory axons of DRG neurons is the major cause of DPN [1]. Although DPN has been intensively studied, molecular mechanisms underlying distal axonal damage have not been fully explored [1, 2]. Emerging experimental and human data suggest that miRNAs are involved in DPN [34]. Patients with T2D exhibit neuropathy susceptibility when they have polymorphisms in miRNA genes such as miR-146a [35]. A recent study in type I diabetic mice shows that DPN significantly alters miRNA profiles including miR-34a in DRG neurons, and that administration of exogenous let-7i miRNA substantially ameliorates DPN by marked augmentation of epidermal nerve fibers [36]. We previously

demonstrated that miR-29c is a negative regulator of axonal growth of DRG neurons by targeting PRKCI under hyperglycemia [33]. The present study shows that attenuation and elevation of miR-34a in DRG neurons promotes and inhibits, respectively, axonal growth under HG condition, providing new evidence that miR-34a mediates axonal growth of sensory neurons. Alteration of miR-34a levels has been associated to diabetes. For example, patients with diabetes have elevated serum levels of miR-34a, while increased miR-34a has been detected in [11] blood, liver and pancreas of diabetic animals [34]. Moreover, miR-34a regulates neurite outgrowth and spinal morphology and function [14].

FOXP2 and *VAT1* are genes putatively targeted by miR-34a based on Targetscan and studies in cancer [37]. We for the first time demonstrated that miR-34a targets a seed region in 3' UTR of *FOXP2* and *VAT1* genes and that downregulation of FOXP2 and VAT1 reduces axonal growth. These findings underscore new function of miR-34a/FXOP2/VAT1 in mediating DPN.

FOXP2 was the first gene found to cause speech and language disorders and autism spectrum disorder [38]. Later studies demonstrated that FOXP2 protein, as a transcription factor, plays important roles in regulating development of the CNS [15]. For example, Groszer et al. reported that a mutation of *FOXP2* leads to abnormal synaptic plasticity in mice [39], while Horng et al. demonstrated that Foxp2 protein is required for synaptic plasticity of the auditory pathway [40]. Others showed that FOXP2 regulates a series of gene networks that are involved in neurite outgrowth in the developing brain [41]. Moreover, a recent study showed that FOXP2 is necessary for glucose metabolism in mediating islet alpha cell proliferation and function [42], suggesting that FOXP2 may have a role in diabetes. The present study shows that FOXP2 in DRG neurons regulated axonal growth. Specifically, we found that hyperglycemia down-regulated *FOXP2* and attenuation of endogenous *FOXP2* resulted in reduction of axonal growth. Thus, in addition to the CNS, FOXP2 regulates peripheral sensory neuron function.

VAT1 was originally described in torpedo fish as an integral membrane protein that plays a central role in the function of synaptic vesicles [16]. Subsequent studies showed that VAT1 is involved in dopamine biosynthesis and synaptic release [43]. The presynaptic release apparatus is highly mobile in axons [44] and axonal transporters of synaptic vesicles mediate autonomic neuropathy [45], suggesting that VAT1 as a synaptic vesicle membrane protein has a role in axonal growth. Moreover, VAT1 possesses ATPase activity [46] that is highly involved in diabetes and diabetic neuropathy [47, 48]. Our findings showed that hyperglycemia downregulated VAT1 expression in DRG neurons, while loss of VAT1 in DRG neurons decreased axonal growth. These findings are in parallel with a role of VAT1 in mediating synaptic function [45–48]. Thus, VAT1 could play a role in DPN.

Collectively, our in vitro and in vivo data for the first time demonstrate that miR-34a mediates axonal growth of DRG neurons by targeting FOXP2 and VAT1 genes under hyperglycemia. However, additional in vivo studies are warranted to investigate whether miR-34a locally regulates FOXP2 and VAT1 protein levels in the distal axons of diabetic mice, as DPN commonly initially damages distal sensory nerve fibers [49].

Supplementary Material

Refer to Web version on PubMed Central for supplementary material.

Acknowledgements

This work was supported by NINDS grants R01 NS075084 (LW) and RO1 NS075156 (ZGZ) and NIDDK RO1 DK097519 (LW). We thank Dr. Paul Fernyhough and colleagues in his laboratory to train us how to culture adult DRG neurons.

References

1. Feldman EL, Nave KA, Jensen TS, Bennett DL (2017) New horizons in diabetic neuropathy: mechanisms, bioenergetics, and pain. Neuron 93(6):1296–1313. 10.1016/j.neuron.2017.02.005 [PubMed: 28334605]
2. Zenker J, Ziegler D, Chrast R (2013) Novel pathogenic pathways in diabetic neuropathy. Trends Neurosci 36(8):439–449. 10.1016/j.tins.2013.04.008 [PubMed: 23725712]
3. Vincent AM, Callaghan BC, Smith AL, Feldman EL (2011) Diabetic neuropathy: cellular mechanisms as therapeutic targets. Nat Rev Neurol 7(10):573–583. 10.1038/nrneurol.2011.137 [PubMed: 21912405]
4. Wang B, Bao L (2017) Axonal microRNAs: localization, function and regulatory mechanism during axon development. J Mol Cell Biol 9(2):82–90. 10.1093/jmcb/mjw050 [PubMed: 27932485]
5. Kantharidis P, Wang B, Carew RM, Lan HY (2011) Diabetes complications: the microRNA perspective. Diabetes 60(7):1832–1837. 10.2337/db11-0082 [PubMed: 21709278]
6. Gong Q, Lu Z, Huang Q, Ruan L, Chen J, Liang Y, Wang H, Yue Y et al. (2015) Altered microRNAs expression profiling in mice with diabetic neuropathic pain. Biochem Biophys Res Commun 456(2): 615–620. 10.1016/j.bbrc.2014.12.004 [PubMed: 25498543]
7. Zhang X, Gong X, Han S, Zhang Y (2014) MiR-29b protects dorsal root ganglia neurons from diabetic rat. Cell Biochem Biophys 70(2): 1105–1111. https://doi.org/10.1007/s 12013-014-0029-y [PubMed: 24819309]
8. Sakai A, Saitow F, Miyake N, Miyake K, Shimada T, Suzuki H (2013) miR-7a alleviates the maintenance of neuropathic pain through regulation of neuronal excitability. Brain : J Neurol 136(Pt 9):2738–2750. 10.1093/brain/awt191
9. Zhou S, Zhang S, Wang Y, Yi S, Zhao L, Tang X, Yu B, Gu X et al. (2015) MiR-21 and miR-222 inhibit apoptosis of adult dorsal root ganglion neurons by repressing TIMP3 following sciatic nerve injury. Neurosci Lett 586:43–49. 10.1016/j.neulet.2014.12.006 [PubMed: 25484256]
10. Hermeking H (2010) The miR-34 family in cancer and apoptosis. Cell Death Differ 17(2):193–199. 10.1038/cdd.2009.56 [PubMed: 19461653]
11. Kong L, Zhu J, Han W, Jiang X, Xu M, Zhao Y, Dong Q, Pang Z et al. (2011) Significance of serum microRNAs in pre-diabetes and newly diagnosed type 2 diabetes: a clinical study. Acta Diabetol 48(1):61–69. 10.1007/s00592-010-0226-0 [PubMed: 20857148]
12. Lovis P, Roggli E, Laybutt DR, Gattesco S, Yang JY, Widmann C, Abderrahmani A, Regazzi R (2008) Alterations in microRNA expression contribute to fatty acid-induced pancreatic beta-cell dysfunction. Diabetes 57(10):2728–2736. 10.2337/db07-1252 [PubMed: 18633110]
13. Rottiers V, Naar AM (2012) MicroRNAs in metabolism and metabolic disorders. Nat Rev Mol Cell Biol 13(4):239–250. 10.1038/nrm3313 [PubMed: 22436747]
14. Agostini M, Tucci P, Steinert JR, Shalom-Feuerstein R, Rouleau M, Aberdam D, Forsythe ID, Young KW et al. (2011) microRNA-34a regulates neurite outgrowth, spinal morphology, and function. Proc Natl Acad Sci U S A 108(52):21099–21104. 10.1073/pnas.1112063108 [PubMed: 22160706]
15. Konopka G, Bomar JM, Winden K, Coppola G, Jonsson ZO, Gao F, Peng S, Preuss TM et al. (2009) Human-specific transcriptional regulation of CNS development genes by FOXP2. Nature 462(7270):213–217. 10.1038/nature08549 [PubMed: 19907493]

16. Linial M, Miller K, Scheller RH (1989) VAT-1: an abundant membrane protein from Torpedo cholinergic synaptic vesicles. Neuron 2(3):1265–1273 [PubMed: 2483112]
17. Wang L, Chopp M, Szalad A, Liu Z, Lu M, Zhang L, Zhang J, Zhang RL et al. (2012) Thymosin beta4 promotes the recovery of peripheral neuropathy in type II diabetic mice. Neurobiol Dis 48(3): 546–555. 10.1016/j.nbd.2012.08.002 [PubMed: 22922221]
18. Chen H, Charlat O, Tartaglia LA, Woolf EA, Weng X, Ellis SJ, Lakey ND, Culpepper J et al. (1996) Evidence that the diabetes gene encodes the leptin receptor: Identification of a mutation in the leptin receptor gene in db/db mice. Cell 84(3):491–495 [PubMed: 8608603]
19. Molliver DC, Wright DE, Leitner ML, Parsadanian AS, Doster K, Wen D, Yan Q, Snider WD (1997) IB4-binding DRG neurons switch from NGF to GDNF dependence in early postnatal life. Neuron 19(4):849–861 [PubMed: 9354331]
20. Hur EM, Yang IH, Kim DH, Byun J, Saijilafu XWL, Nicovich PR, Cheong R, Levchenko A et al. (2011) Engineering neuronal growth cones to promote axon regeneration over inhibitory molecules. Proc Natl Acad Sci U S A 108(12):5057–5062. 10.1073/pnas.1011258108 [PubMed: 21383151]
21. Taylor AM, Blurton-Jones M, Rhee SW, Cribbs DH, Cotman CW, Jeon NL (2005) A microfluidic culture platform for CNS axonal injury, regeneration and transport. Nat Methods 2(8):599–605. 10.1038/nmeth777 [PubMed: 16094385]
22. Russell JW, Sullivan KA, Windebank AJ, Herrmann DN, Feldman EL (1999) Neurons undergo apoptosis in animal and cell culture models of diabetes. Neurobiol Dis 6(5):347–363. 10.1006/nbdi.1999.0254 [PubMed: 10527803]
23. Jia L, Wang L, Chopp M, Zhang Y, Szalad A, Zhang ZG (2016) MicroRNA 146a locally mediates distal axonal growth of dorsal root ganglia neurons under high glucose and sildenafil conditions. Neuroscience 329:43–53. 10.1016/j.neuroscience.2016.05.005 [PubMed: 27167084]
24. Wang L, Chopp M, Szalad A, Zhang Y, Wang X, Zhang RL, Liu XS, Jia L et al. (2014) The role of miR-146a in dorsal root ganglia neurons of experimental diabetic peripheral neuropathy. Neuroscience 259:155–163. https://doi.org/10.1016Zj.neuroscience.2013.11.057 [PubMed: 24316060]
25. Zhang Y, Ueno Y, Liu XS, Buller B, Wang X, Chopp M, Zhang ZG (2013) TheMicroRNA-17-92 cluster enhances axonal outgrowth in embryonic cortical neurons. J Neurosci : Off J Soc Neurosci 33(16): 6885–6894. 10.1523/JNEUROSCI.5180-12.2013
26. Livak KJ, Schmittgen TD (2001) Analysis of relative gene expression data using real-time quantitative PCR and the 2(-Delta Delta C(T)) method. Methods 25(4):402–408 [PubMed: 11846609]
27. Zhang Y, Chopp M, Liu XS, Kassis H, Wang X, Li C, An G, Zhang ZG (2015) MicroRNAs in the axon locally mediate the effects of chondroitin sulfate proteoglycans and cGMP on axonal growth. Dev Neurobiol 75(12):1402–1419. 10.1002/dneu.22292 [PubMed: 25788427]
28. Saijilafu HEM, Liu CM, Jiao Z, Xu WL, Zhou FQ (2013) PI3K-GSK3 signalling regulates mammalian axon regeneration by inducing the expression of Smad1. Nat Commun 4:2690 10.1038/ncomms3690 [PubMed: 24162165]
29. Lupachyk S, Watcho P, Shevalye H, Vareniuk I, Obrosov A, Obrosova IG, Yorek MA (2013) Na +/H+ exchanger 1 inhibition reverses manifestation of peripheral diabetic neuropathy in type 1 diabetic rats. Am J Phys Endocrinol Metab 305(3):E396–E404. 10.1152/ajpendo.00186.2013
30. Liu XS, Chopp M, Pan WL, Wang XL, Fan BY, Zhang Y, Kassis H, Zhang RL et al. (2016) MicroRNA-146a promotes oligodendrogenesis in stroke. Mol Neurobiol 54:227–237. 10.1007/s12035-015-9655-7 [PubMed: 26738853]
31. Lewis BP, Shih IH, Jones-Rhoades MW, Bartel DP, Burge CB (2003) Prediction of mammalian microRNA targets. Cell 115(7): 787–798 [PubMed: 14697198]
32. Xu XH, Deng CY, Liu Y, He M, Peng J, Wang T, Yuan L, Zheng ZS et al. (2014) MARCKS regulates membrane targeting of Rab10 vesicles to promote axon development. Cell Res 24(5): 576–594. 10.1038/cr.2014.33 [PubMed: 24662485]
33. Jia L, Wang L, Chopp M, Li C, Zhang Y, Szalad A, Zhang ZG (2017) MiR-29c/PRKCI regulates axonal growth of dorsal root ganglia neurons under hyperglycemia. Mol Neurobiol 55:851–858. 10.1007/s12035-016-0374-5 [PubMed: 28070856]

34. Zhu H, Leung SW (2015) Identification of microRNA biomarkers in type 2 diabetes: a meta-analysis of controlled profiling studies. Diabetologia 58(5):900–911. 10.1007/s00125-015-3510-2 [PubMed: 25677225]
35. Ciccacci C, Morganti R, Di Fusco D, D'Amato C, Cacciotti L, Greco C, Rufini S, Novelli G et al. (2014) Common polymorphisms in MIR146a, MIR128a and MIR27a genes contribute to neuropathy susceptibility in type 2 diabetes. Acta Diabetol 51(4):663–671. 10.1007/s00592-014-0582-2 [PubMed: 24682535]
36. Cheng C, Kobayashi M, Martinez JA, Ng H, Moser JJ, Wang X, Singh V, Fritzler MJ et al. (2015) Evidence for epigenetic regulation of gene expression and function in chronic experimental diabetic neuropathy. J Neuropathol Exp Neurol 74(8):804–817. 10.1097/NEN.0000000000000219 [PubMed: 26172287]
37. Cuiffo BG, Campagne A, Bell GW, Lembo A, Orso F, Lien EC, Bhasin MK, Raimo M et al. (2014) MSC-regulated microRNAs converge on the transcription factor FOXP2 and promote breast cancer metastasis. Cell Stem Cell 15(6):762–774. 10.1016/j.stem.2014.10.001 [PubMed: 25515522]
38. Vernes SC, Newbury DF, Abrahams BS, Winchester L, Nicod J, Groszer M, Alarcon M, Oliver PL et al. (2008) A functional genetic link between distinct developmental language disorders. N Engl J Med 359(22):2337–2345. 10.1056/NEJMoa0802828 [PubMed: 18987363]
39. Groszer M, Keays DA, Deacon RM, de Bono JP, Prasad-Mulcare S, Gaub S, Baum MG, French CA, Nicod J, Coventry JA, Enard W, Fray M, Brown SD, Nolan PM, Paabo S, Channon KM, Costa RM, Eilers J, Ehret G, Rawlins JN, Fisher SE (2008) Impaired synaptic plasticity and motor learning in mice with a point mutation implicated in human speech deficits. Curr Biol : CB 18 (5): 354–362. doi: 10.1016/j.cub.2008.01.060 [PubMed: 18328704]
40. Horng S, Kreiman G, Ellsworth C, Page D, Blank M, Millen K, Sur M (2009) Differential gene expression in the developing lateral geniculate nucleus and medial geniculate nucleus reveals novel roles for Zic4 and Foxp2 in visual and auditory pathway development. J Neurosci: Off J Soc Neurosci 29(43):13672–13683. 10.1523/JNEUROSCI.2127-09.2009
41. Vernes SC, Oliver PL, Spiteri E, Lockstone HE, Puliyadi R, Taylor JM, Ho J, Mombereau C et al. (2011) Foxp2 regulates gene networks implicated in neurite outgrowth in the developing brain. PLoS Genet 7(7):e1002145 10.1371/journal.pgen.1002145 [PubMed: 21765815]
42. Spaeth JM, Hunter CS, Bonatakis L, Guo M, French CA, Slack I, Hara M, Fisher SE et al. (2015) The FOXP1, FOXP2 and FOXP4 transcription factors are required for islet alpha cell proliferation and function in mice. Diabetologia 58(8):1836–1844. https://doi.org/10. 1007/s00125-015-3635-3 [PubMed: 26021489]
43. Ma Z, Guo W, Guo X, Wang X, Kang L (2011) Modulation of behavioral phase changes of the migratory locust by the catecholamine metabolic pathway. Proc Natl Acad Sci U S A 108(10): 3882–3887. 10.1073/pnas.1015098108 [PubMed: 21325054]
44. Krueger SR, Kolar A, Fitzsimonds RM (2003) The presynaptic release apparatus is functional in the absence of dendritic contact and highly mobile within isolated axons. Neuron 40(5):945–957 [PubMed: 14659093]
45. Riviere JB, Ramalingam S, Lavastre V, Shekarabi M, Holbert S, Lafontaine J, Srour M, Merner N et al. (2011) KIF1A, an axonal transporter of synaptic vesicles, is mutated in hereditary sensory and autonomic neuropathy type 2. Am J Hum Genet 89(2):219–230. 10.1016/j.ajhg.2011.06.013 [PubMed: 21820098]
46. Hayess K, Kraft R, Sachsinger J, Janke J, Beckmann G, Rohde K, Jandrig B, Benndorf R (1998) Mammalian protein homologous to VAT-1 of Torpedo californica: isolation from Ehrlich ascites tumor cells, biochemical characterization, and organization of its gene. J Cell Biochem 69(3):304–315 [PubMed: 9581869]
47. Bidasee KR, Zhang Y, Shao CH, Wang M, Patel KP, Dincer UD, Besch HR, Jr (2004) Diabetes increases formation of advanced glycation end products on Sarco(endo)plasmic reticulum Ca2+-ATPase. Diabetes 53(2):463–473 [PubMed: 14747299]
48. Calcutt NA, Tomlinson DR, Biswas S (1990) Coexistence of nerve conduction deficit with increased Na(+)-K(+)-ATPase activity in galactose-fed mice. Implications for polyol pathway and diabetic neuropathy Diabetes. 39(6):663–666 [PubMed: 2161366]

49. Peltier A, Goutman SA, Callaghan BC (2014) Painful diabetic neuropathy. BMJ 348:g1799 10.1136/bmj.g1799 [PubMed: 24803311]

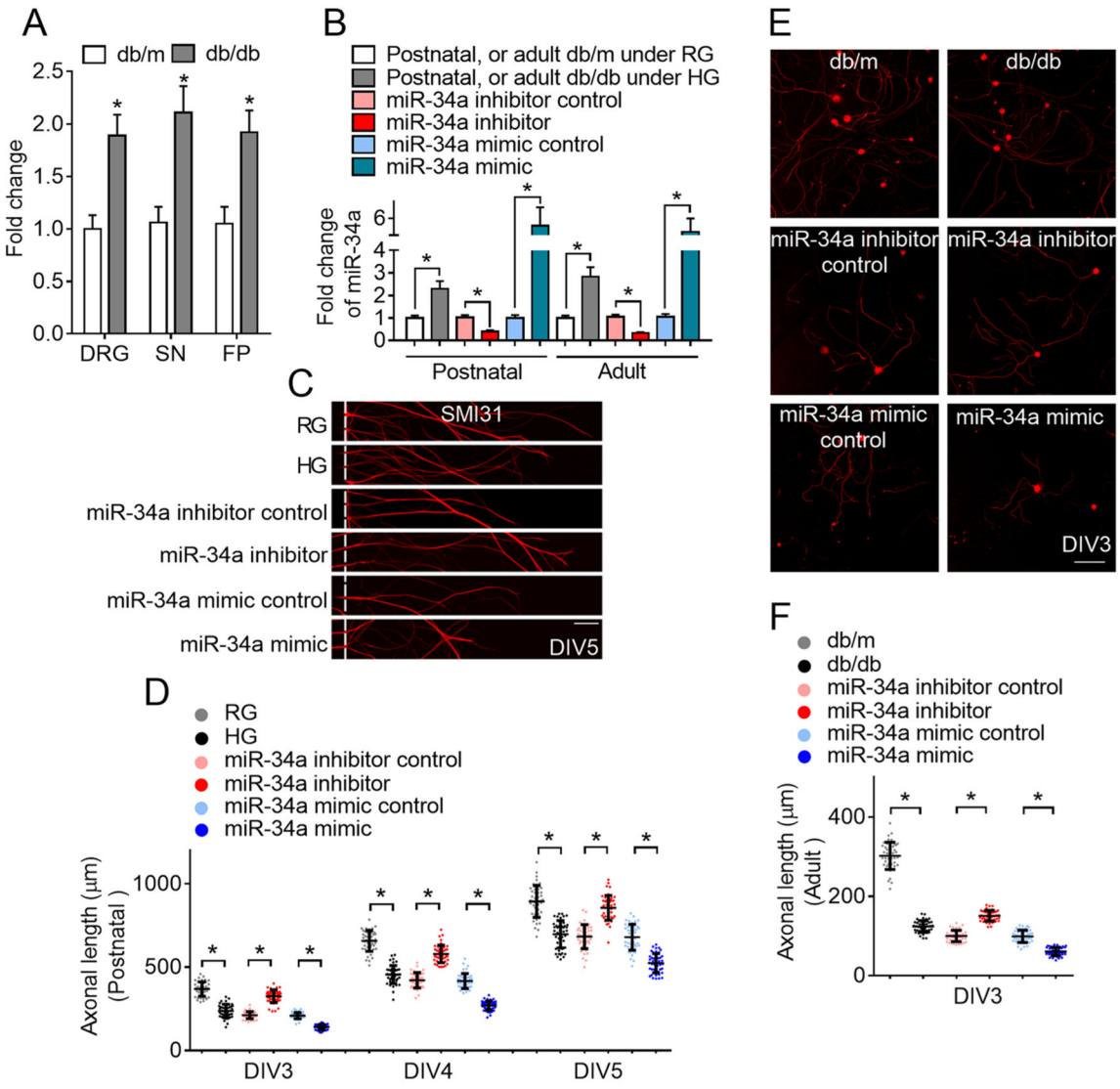

Fig. 1.

Role of miR-34a in regulating axonal growth. **a** qRT-PCR data show miR-34a levels in DRG, sciatic nerve and foot pad tissues of db/db or db/m mice. **b** qRT-PCR data show miR-34a levels in postnatal or adult DRG neurons cultured under regular glucose (RG) or high glucose (HG) conditions and in DRG neurons transfected with miR-34a inhibitors, miR-34a mimics, or their corresponding controls. Adult DRG neurons were isolated from 20 weeks old db/m or db/db mice. **c** Representative microscopic images of SMI31+ axons (Red) of postnatal DRG neurons transfected with miR-34a inhibitor, miR-34a mimic, or their corresponding controls under HG condition. **d** Quantitative data show axonal lengths of postnatal neurons under various conditions. **e**, **f** Representative microscopic images (**e**) and quantitative data (**f**) show TUJ1+ neurite lengths of adult DRG neurons under various conditions. $n = 6$ mice/group (**a**, **b**), 45 axons/3 chambers/3 individual experiments /group (**d**) or 20 neurons/3 dishes/group (**f**). $*P < 0.05$. Scale bar= 100 μm (**c**), or 50 μm (**e**)

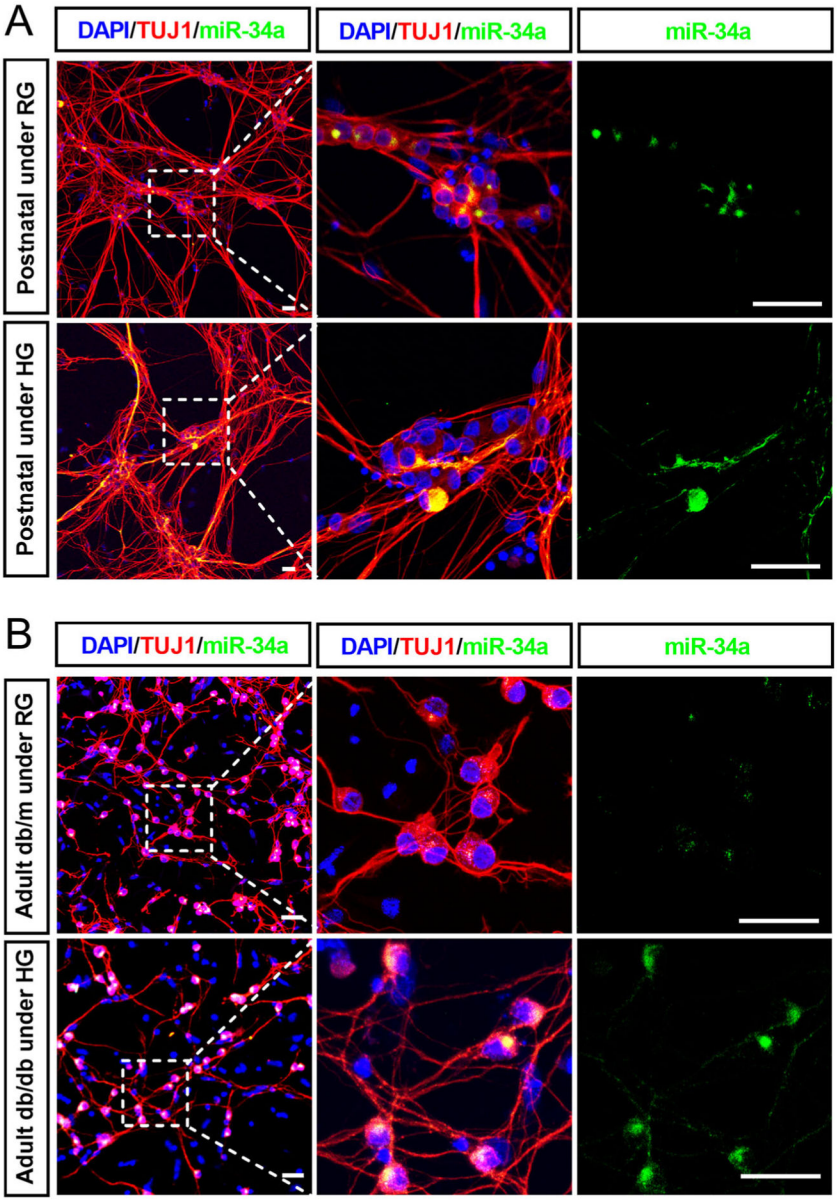

Fig. 2.

MiR-34a in cultured postnatal and adult DRG neurons. **a** Representative images of FISH in combination with immunofluorescent staining show increased miR-34a signals (green) in TUJ1+ postnatal DRG neurons (red) cultured under HG compared to neurons under RG. **b** Representative images of FISH in combination with immunofluorescent staining show increased miR-34a signals (green) in TUJ1+ adult DRG neurons (red) from db/db under HG compared to adult DRG neurons from db/m under RG. Scale bar = 50 μm

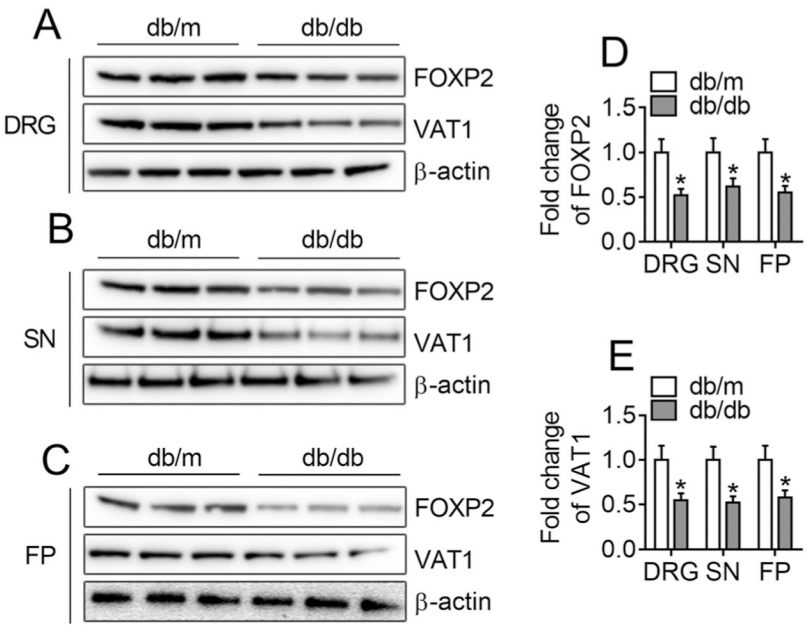

Fig. 3.

Reduction of FOXP2 and VAT1 proteins in diabetic mouse tissues. **a–c** Representative Western blots show protein levels of FOXP2 and VAT1 in DRG (**a**), sciatic nerve (SN, **b**) and foot pad (FP, **c**) tissues of db/db or db/m mice. Three individual mice were presented for each group and β-actin was used as an internal loading control. **d**, **e** Quantitative data show levels of FOXP2 (**d**) and VAT1 (**e**) in DRG, SN and FP. $n = 6$ mice/group. $*P < 0.05$ vs db/m mice

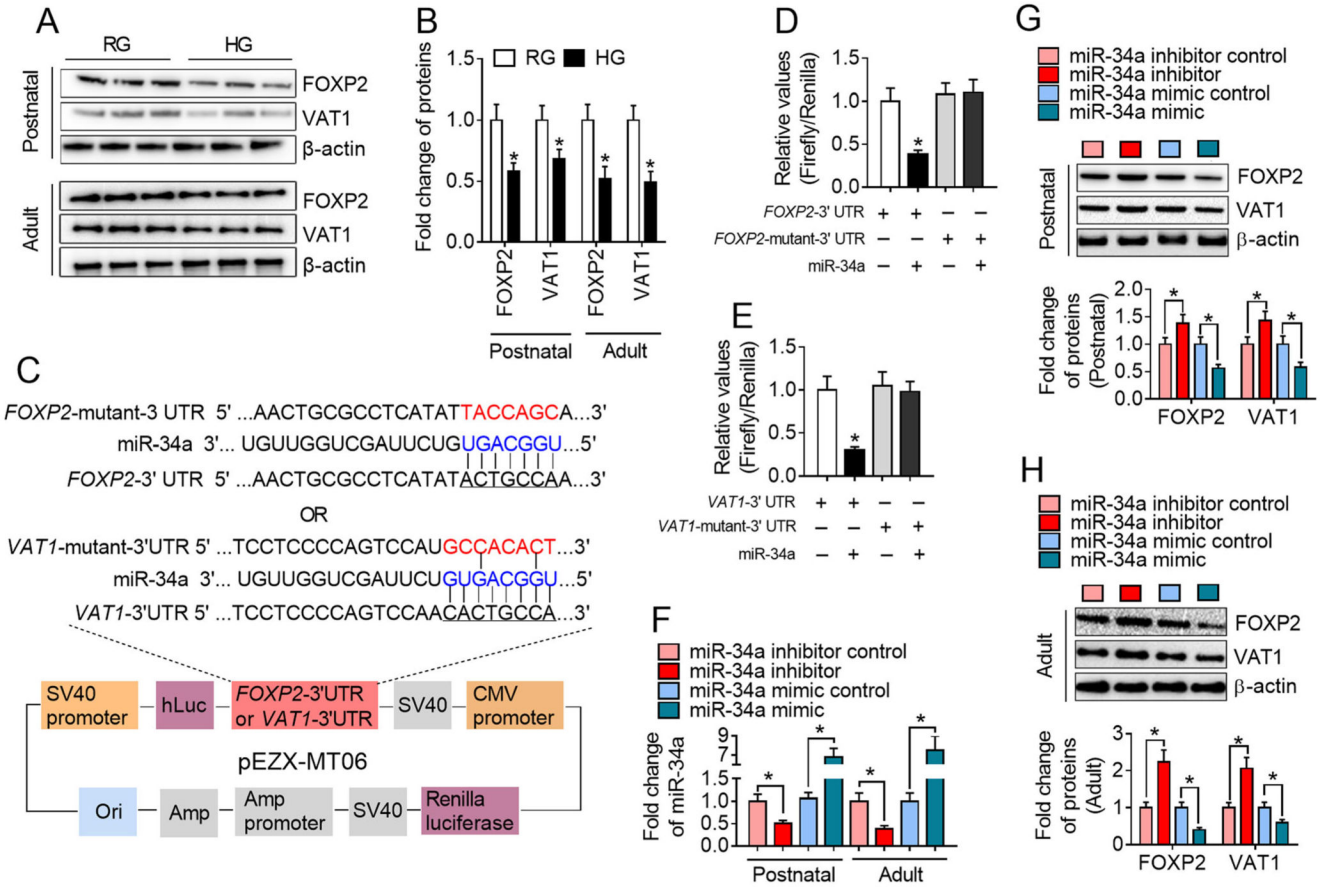

Fig. 4.

MiR-34a regulates FOXP2 or VAT1 genes by targeting their 3′ UTR. **a**, **b** Representative Western blots (**a**) and their quantitative data (**b**) show levels of FOXP2 and VAT1 in postnatal and adult DRG neurons cultured under RG and HG conditions. **c** A schematic illustration shows the dual-luciferase reporter vector cloned with wild type or mutant 3′ UTR of FOXP2 or VAT1. **d**, **e** Quantitative luciferase data show the activity of wild type or mutant 3′ UTR of FOXP2 (**d**) or VAT1 (**e**) with and without miR-34a mimic. **f** qRT-PCR data show miR-34a levels in postnatal and adult DRG neurons transfected with the miR-34a inhibitor or mimics, and their corresponding controls under HG condition. **g**, **h** Representative Western blots and their quantitative data show levels of FOXP2 and VAT1 in postnatal (**g**) and adult (**h**) DRG neurons transfected with the miR-34a inhibitor or mimics, and their corresponding controls under high glucose (HG) condition. $n = 6$ chambers/3 individual experiments/group (**a-b**, **f-h**) or 6 wells/3 individual experiments/group (**d-e**) $^*P < 0.05$

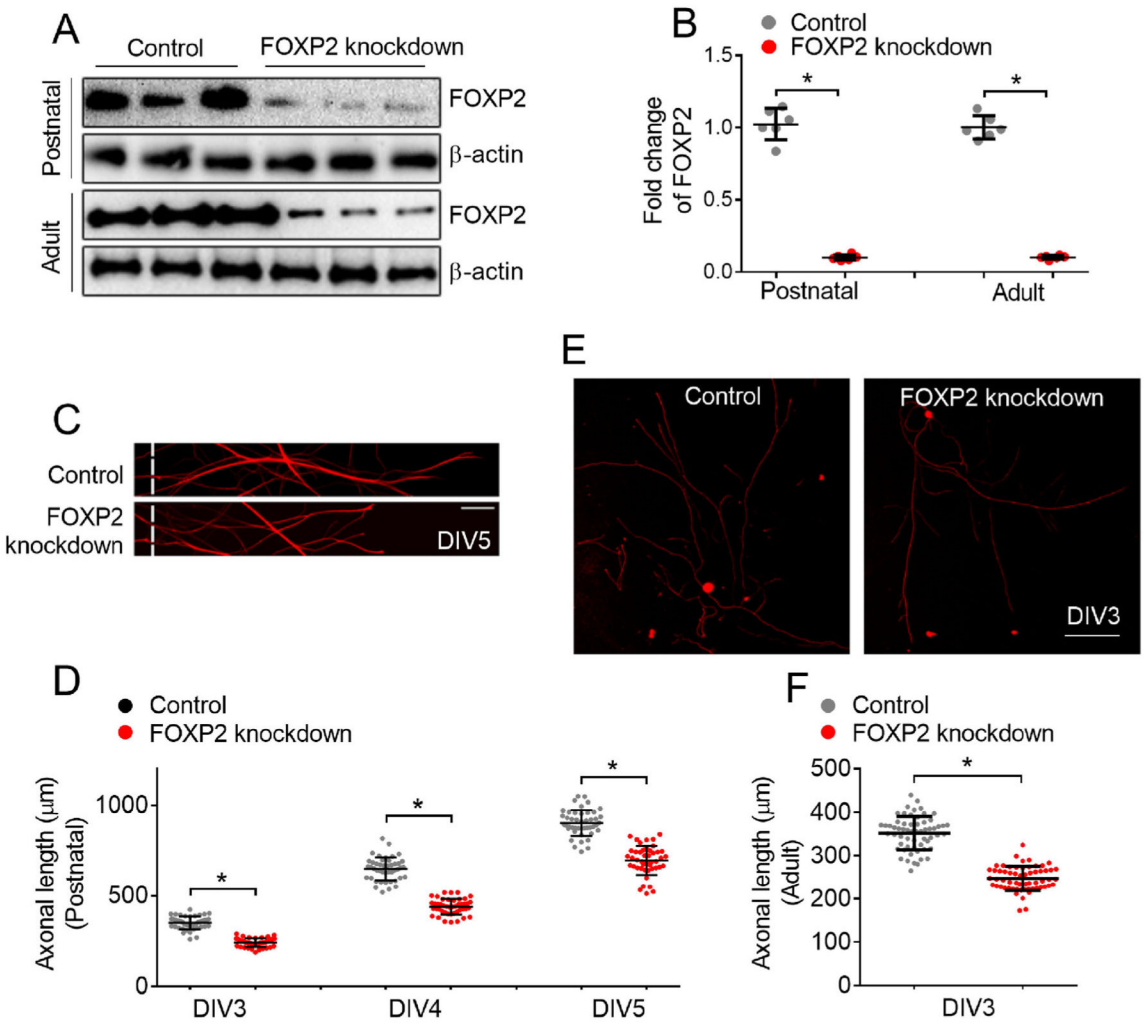

Fig. 5.

Attenuation of endogenous FOXP2 in DRG neurons reduces axonal growth. **a-b** Representative Western blots (**a**) and their quantitative data (**b**) show levels of FOXP2 in postnatal and adult DRG neurons transfected with siRNA against FOXP2 (FOXP2 knockdown). **c-d** Representative microscopic images (**c**) and quantitative data (**d**) show SMI31+ (red) axonal length of postnatal DRG neurons transfected with siRNA against FOXP2 (FOXP2 knockdown) under RG conditions. **e-f** Representative microscopic images (**e**) and quantitative data (**f**) show TUJ1+ axonal length of adult DRG neurons transfected with siRNA against FOXP2 (FOXP2 knockdown) under RG conditions. $n = 6$ chambers or dishes/3 individual experiments /group (**a-b**), 45 axons/3 chambers/3 individual experiments /group (**d**) or 20 neurons /3 dishes/group (**f**). $*P < 0.05$. Scale bar= 100 μm (**c**), or 50 μm (**e**)

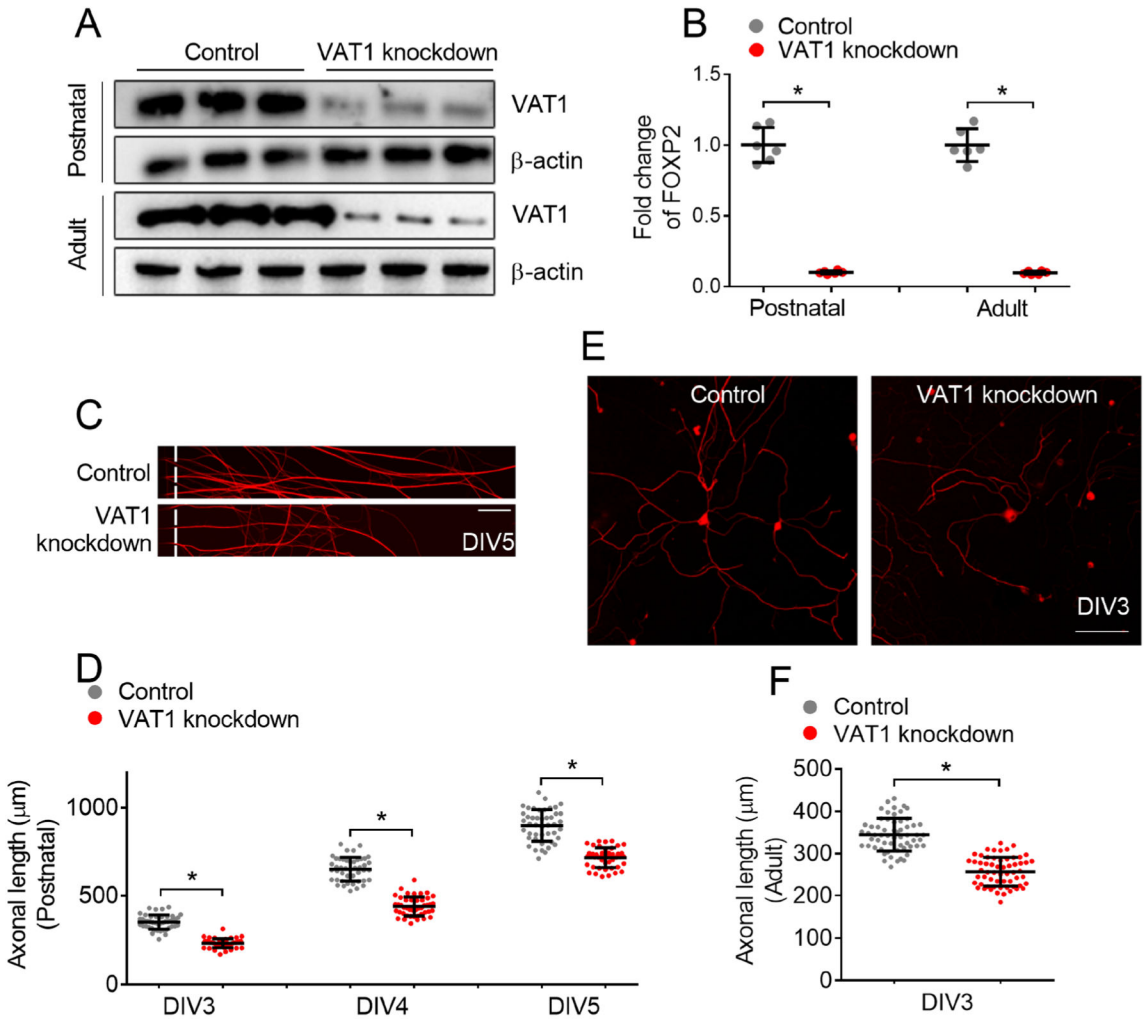

Fig. 6.

Attenuation of endogenous VAT1 in DRG neurons reduces axonal growth. **a-b** Representative Western blots (**a**) and their quantitative data (**b**) show levels of VAT1 in postnatal and adult DRG neurons transfected with siRNA against VAT1 (VAT1 knockdown). **c-d** Representative microscopic images (**c**) and quantitative data (**d**) show SMI31 + axonal length of postnatal DRG neurons transfected with siRNA against VAT1 (VAT1 knockdown) under RG conditions. **e-f** Representative microscopic images (**e**) and quantitative data (**f**) show TUJ1+ axonal length of adult DRG neurons transfected with siRNA VAT1 (VAT1 knockdown) under RG conditions. $n = 6$ chambers or dishes/3 individual experiments /group (**a-b**), 45 axons/3 chambers/3 individual experiments /group (**d**) or 20 neurons/3 dishes/ group (**f**).*$P < 0.05$. Scale bar= 100 μm (**c**), or 50 μm (**e**)